Canadian Geotechnical Journal. Submitted 17 June 2018; accepted 27 June 2019.
https://doi.org/10.1139/cgj-2018-0398

Creep and consolidation of a stiff clay under saturated and unsaturated conditions

Mohammad Rezania, Meghdad Bagheri, Mohaddeseh Mousavi Nezhad

Mohammad Rezania PhD
Associate Professor, School of Engineering, University of Warwick, Coventry, UK
Email: m.rezania@warwick.ac.uk (Corresponding author)
Phone: +44 (0)24 76 522339
Fax: +44 (0)24 76 524560

Meghdad Bagheri PhD
Lecturer, School of Energy, Construction and Environment, Coventry University, Coventry, UK
Email: ac6031@coventry.ac.uk

Mohaddeseh Mousavi Nezhad PhD
Associate Professor, School of Engineering, University of Warwick, Coventry, UK
Email: m.mousavi-nezhad@warwick.ac.uk

Canadian Geotechnical Journal. Submitted 17 June 2018; accepted 27 June 2019.
https://doi.org/10.1139/cgj-2018-0398

Abstract

In this paper the one-dimensional (1D) time-dependent behaviour of natural and reconstituted London Clay samples under saturated and unsaturated conditions is studied. For this purpose, a set of 1D consolidation tests including multi-staged loading (MSL) oedometer tests and single-staged loading (SSL) long-term oedometer creep tests were carried out on saturated and unsaturated specimens. Conventional oedometer cells were used for tests on saturated specimens, whereas a newly designed unsaturated oedometer cell, equipped with two high-capacity tensiometers (HCTs) for suction measurements, was used for unsaturated tests. The tests results revealed stress- and suction-dependency of primary and secondary consolidation responses of the soil samples. Furthermore, counter to formerly acknowledged suggestions of independency of the slope of normal consolidation line to suction changes, it was observed that an increase in suction results in a decrease of the slope of compression curve (C_c) and the creep index ($C_{\alpha e}$) values, and an increase in yield vertical net stress (σ_p). Moreover, the $C_{\alpha e}/C_c$ ratio for London Clay was found to be stress- and suction-dependent, unlike the previously suggested hypotheses.

Keywords: Stiff clay, Creep, Oedometer, Suction, Unsaturated soils

Canadian Geotechnical Journal. Submitted 17 June 2018; accepted 27 June 2019.
https://doi.org/10.1139/cgj-2018-0398

Introduction

Experimental investigations have proven dependency of the mechanical behaviour of clays on time effects (Li et al. 2003; Mesri 2009; Karstunen and Yin 2010; Bagheri et al. 2015; Yin and Feng 2017; Rezania et al. 2017; Bagheri et al. 2019*b*). These effects are commonly observed as post-construction deformations of geostructures such as roads, railways, and dams. The time-dependency of mechanical response is usually observed through irreversible creep deformations which are typically coupled with external sources of deformations driven by, for example, repeated loadings, rainfalls, flooding, and earthquakes (Oldecop and Alonso 2007). The main focus of the reported works in the literature has been laid on characterisation of creep deformations in saturated soft clays. This is while the shallow depth soil layers, typically studied for practical engineering purposes, are usually found in partially-saturated states. Little is currently known about the compression and creep response of unsaturated clays, in particular stiff clays such as London Clay (LC). The reported works on creep response in unsaturated conditions are limited to observations of time-dependent volume change behaviour of reservoir chalks (De Gennaro et al. 2003; De Gennaro et al. 2005; Priol et al. 2007; Pereira and De Gennaro 2010), rockfills (Oldecop and Alonso 2007), and reconstituted clays (Lai et al. 2010; Nazer and Tarantino 2016). Priol et al. (2007) performed a set of multi-staged loading creep oedometer tests on oil-saturated, water-saturated, partially-saturated, and dry Lixhe chalk (an outcrop chalk from Belgium) and reported that at high pressures the creep index ($C_{\alpha e}$) values increased with increase in vertical stress and decreased with increase in suction (s). Similar results were reported by De Gennaro et al. (2005) who evaluated the suction- and stress-dependency of creep index in MSL compression tests on Estreux chalk under dry, water-saturated, and unsaturated (s = 1.5 MPa) conditions using a suction-controlled osmotic oedometer cell. The results of unsaturated triaxial drained creep tests performed on sliding zone soils of the Qianjiangping landslide (Lai et al. 2010) demonstrated that an increase in matric suction results in a decrease in creep strain rate and magnitude under constant

net confining pressure and deviatoric stress. However, despite practical interests, generalisation of these findings to various soil types, stress states, and suction ranges and coupling partial saturation states and time effects is still an open topic.

This paper presents the results of multi-staged loading (MSL) and single-stage loading (SSL) oedometer creep tests performed on saturated and unsaturated LC specimens. Saturated tests were performed on undisturbed and reconstituted specimens, whereas the unsaturated creep tests were performed only on reconstituted specimens. The results of MSL tests are discussed with emphasis on the effects of soil structure, suction, and vertical stress level on the compression response, consolidation indices, and $C_{\alpha e}/C_c$ ratio. The effects of suction and vertical stress level on volumetric creep strains are further discussed based on the results of SSL oedometer tests.

Material and Apparatus

The test material is London Clay extracted from the New Hook Farm in Isle of Sheppey in the UK. Undisturbed block samples of un-weathered LC were taken at 4 m depth below non-quarried ground level. The index parameters and physical properties of the natural samples are summarised in Table 1. Laboratory determination of index parameters confirmed the upper bound values of 24% and 78% for respectively plastic limit (w_P) and liquid limit (w_L) indices. Based on the USCS classification, the samples are classified as clay of high plasticity (CH).

The particle size distribution (PSD) curve of natural LC presents 98% particles passing through the 0.063 mm sieve. The high content of fine grain inclusions results in an air-entry value (AEV) of several megapascals (e.g. Monroy et al. 2008). In order to decrease the AEV, the PSD was modified by including larger sized aggregates, resulting from crushing the oven-dried samples, and passing through 1.18 mm sieve. The soil water retention curve (SWRC) and AEV of the sample with modified PSD were measured using axis-translation and high-capacity tensiometer

(HCT) techniques following the procedure outlined in Bagheri et al. (2019*a*). As shown in Fig. 1, the modified sample exhibited an AEV of around 260 kPa which allows for testing specimens over a wider range of suctions lying on the transition (de-saturation) phase of the SWRC. It must be noted here that, although it is desired to obtain the AEV from a plot of degree of saturation versus suction, reliable values for the AEV can be also derived from the plot of water content versus suction (Fredlund 2006).

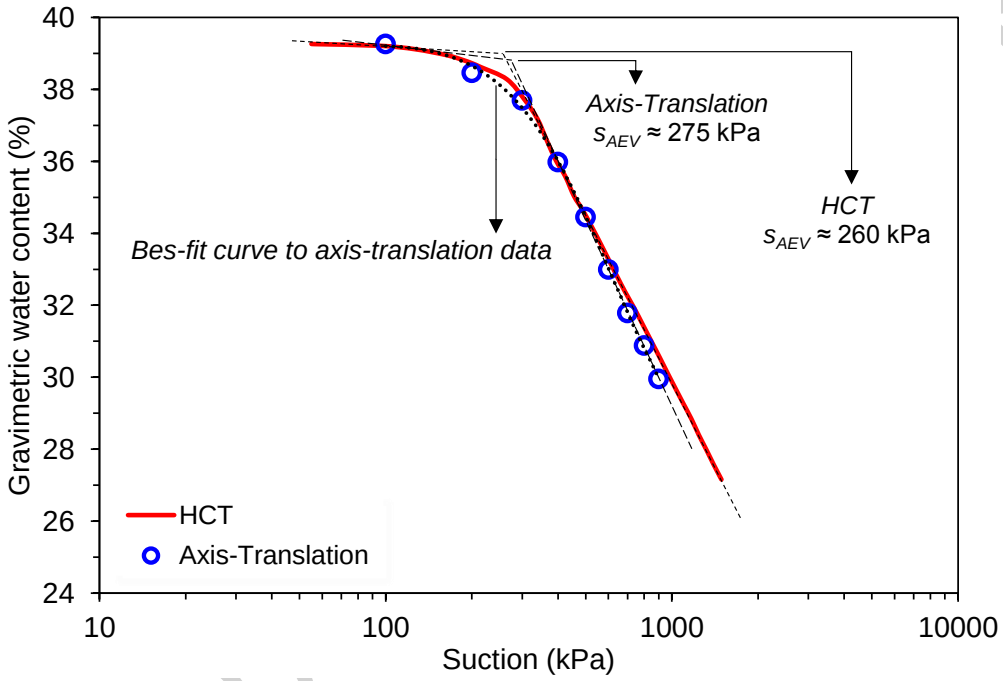

Fig. 1 SWRC determined for main drying path

Undisturbed oedometer specimens were directly cored from the block samples using a 75 mm diameter and 20 mm high oedometer ring. The inner wall of the ring was slightly lubricated with grease before preparing the specimen, in order to minimise the side friction effects on the stress–strain response. Reconstituted soil samples were prepared by mixing the soil powder, containing the large-sized aggregates, with distilled water at $1.5w_L$. The slurry was then consolidated in a 100 mm diameter Perspex consolidometer under a vertical stress of 80 kPa for a duration of 5 days. The samples were then quickly unloaded to minimise swelling and water absorption. Reconstituted saturated specimens were cored from the obtained cylindrical soil cakes. Unsaturated specimens

were cored from smaller subsamples air-dried at room temperature to pre-specified water contents and stored in air-tight containers for a duration of one week to attain moisture equilibrium. Selection of the initial water contents (w_0) of the specimens was based on the information obtained from the developed SWRC for reconstituted samples and to examine compressibility of specimens with a wide range of suctions on the transition effect zone (partially saturated zone) of the main drying curve.

Saturated tests were carried out in conventional oedometer cells, whereas unsaturated tests were carried out in suction-monitored oedometer cells equipped with two high-capacity tensiometers (HCTs) for monitoring suction evolutions (Bagheri et al. 2018). The special design of the oedometer loading cap allows for replacement of a cavitated HCT without any disturbance to the specimen and interruption in measurement of deformations. A schematic view of the unsaturated oedometer cell is provided in Fig. 2.

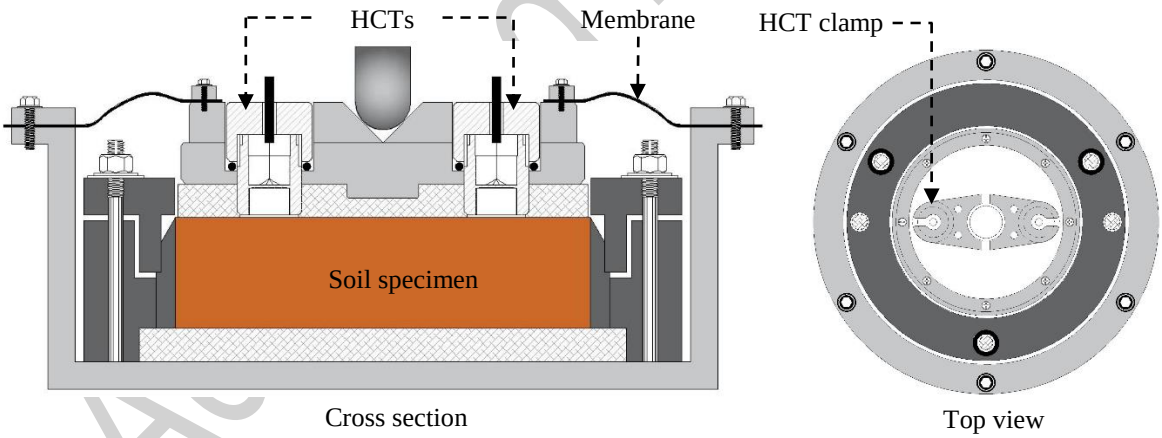

Fig. 2. Schematic diagram of the unsaturated oedometer cell

Experimental Program

MSL oedometer tests with 24 hour loading periods were performed on intact, reconstituted, and low-quality undisturbed (LQU) specimens. Considering the fissured nature of the LC, significant attention was given during the preparation of intact specimens. Where the specimen preparation

process involved minor visible damage to the soil structure, the prepared specimen was marked as LQU. Prior to the start of the tests, the w_0 and the specimen dimensions were measured for saturated MSL tests. The specimen was then set in the conventional oedometer cell and vertical load was applied step-wise to the submerged specimen during each 24 hours loading step. Typically, for conventional oedometer tests, vertical load is doubled at each stage of loading. This can, however, cause significant unfavourable disturbance to the structural properties of the test specimen especially at high stress levels. In order to reduce such effects, in addition to the doubling vertical stress method, other loading patterns, as shown in Table 2, were also considered. By the end of loading to the desired stress levels, the specimens were unloaded step-wise in order to evaluate the swelling response. Each unloading stage was kept for 24 hours to ensure complete swelling and that most of the generated suction was released. The compression curves were finally obtained based on the final settlement values. For unsaturated MSL tests, prior to each experiment, the HCTs were saturated and preconditioned following the procedure explained by Bagheri et al. (2018). In order to ensure ultimate contact between the specimen and the HCTs, the ceramic disks of the tensiometers were covered with soil paste, and a small vertical stress was also applied to the specimen. The average suction recorded by the two HCTs, used to monitor suction changes, at the start of loading was considered as the initial suction (s_0) of the specimen. In all experiments, the pressure difference recorded by the two HCTs did not exceed 5 kPa. The HCTs were also periodically calibrated in order to account for any possible changes in their performance. For specimens with s_0 values beyond the capacity of the HCTs, the corresponding s_0 values were estimated from the curve fitting of the experimental SWRC using Fredlung and Xing (1994) equation. Table 2 presents the details of MSL tests.

SSL tests were carried out only on reconstituted specimens in order to avoid the complexities associated with coupled effects of suction and soil structure. Unlike conventional incremental loading tests, the test pressure was applied directly in a single loading stage in order to remove the

possible effects of loading and creep history on the measured creep strains. Moreover, in order to avoid the problems associated with sudden loading, the applied pressure was ramped up to the desired vertical stress level at a constant rate of 8-10 kPa per hour. The applied pressure was sustained for a period of 19 to 94 days. The values of the maximum applied vertical stresses (σ_{vm}) were chosen so that they were higher than the preconsolidation pressure of the samples so that it was possible to investigate the creep response in the normal consolidation state. Unsaturated tests were conducted on specimens having initial suction states on the main drying curve of the SWRC in order to eliminate the complexity associated with volumetric deformation due to wetting (wetting-induced deformations or collapse in wetting), and therefore observe the effect of suction on mechanically induced creep deformations. Details of the carried out experiments are summarised in Table 3.

Results

The compression index (C_c), swelling index (C_s), and reloading index (C_r) values were calculated as the slope of respectively the normal compression line (NCL), the swelling (unloading) line, and the reloading line of the compression curve plotted in e – log σ'_v space, where e is void ratio and σ'_v is vertical effective stress. As suggested by Mataic et al. (2016), the creep index ($C_{\alpha e}$) was defined as the slope of the plot of void ratio versus logarithm of time (t) from the time period of 6–24 hours for each load increment. The decrease in void ratio during this time scale represents the creep phase as the end of primary consolidation (EOP) was found to be within the first 5–6 hours of each loading increment. The experimental results of unsaturated oedometer tests can be evaluated based on the generalised vertical effective stress relationship;

$$\sigma'_v = \sigma_{vnet} + S_r s \quad (1)$$

where S_r is the degree of saturation, s is soil suction, and $\sigma_{vnet} = \sigma_v - u_a$ is the net normal stress defined as the difference of vertical total stress (σ_v) and pore-air pressure (u_a). Estimation of S_r requires the information of the water content of the specimen during the test. However, as the suction-monitored oedometer cell does not allow for measurement of the specimens' water content, the experimental results of unsaturated oedometer tests were evaluated based on the σ_{vnet}, and since the tests were carried out at the atmospheric air pressure, $\sigma_{vnet} = \sigma_v$.

Evaluation of Compressibility in MSL Tests

A comparison of the normalised compression curves for Sheppey LC and the natural LC from Unit C (block sample retrieved from 5–10 m depth) of the Heathrow Terminal 5 site (T5) (Gasparre 2005) is shown in Fig. 3. The curves exhibited very similar characteristics with almost equal compression and swelling indices. The specimen from T5, however, is less compressible than the Sheppey specimen, mainly due to its lower plasticity index (I_p = 37%) and initial water content (w_0 = 24%). Moreover, the change in loading pattern, which was aimed at reducing the effects of sudden loading and subsequent damages to the soil structure, did not have a notable influence on the obtained compression curves. The only exception was the MSLis32-5 curve which was slightly shifted to the right, and exhibited lower compressibility which could be due to a lower S_r of the specimen at the start of the test. Furthermore, the highly structured nature of the specimens resulted in high C_s values. Similar observations were also reported by Gasparre (2005) for LC samples retrieved from T5. Average C_c and C_s values of respectively 0.218 and 0.096 were obtained from the compression tests on intact specimens having an average initial void ratio of e_0 = 0.85 and initial water content of w_0 = 32%.

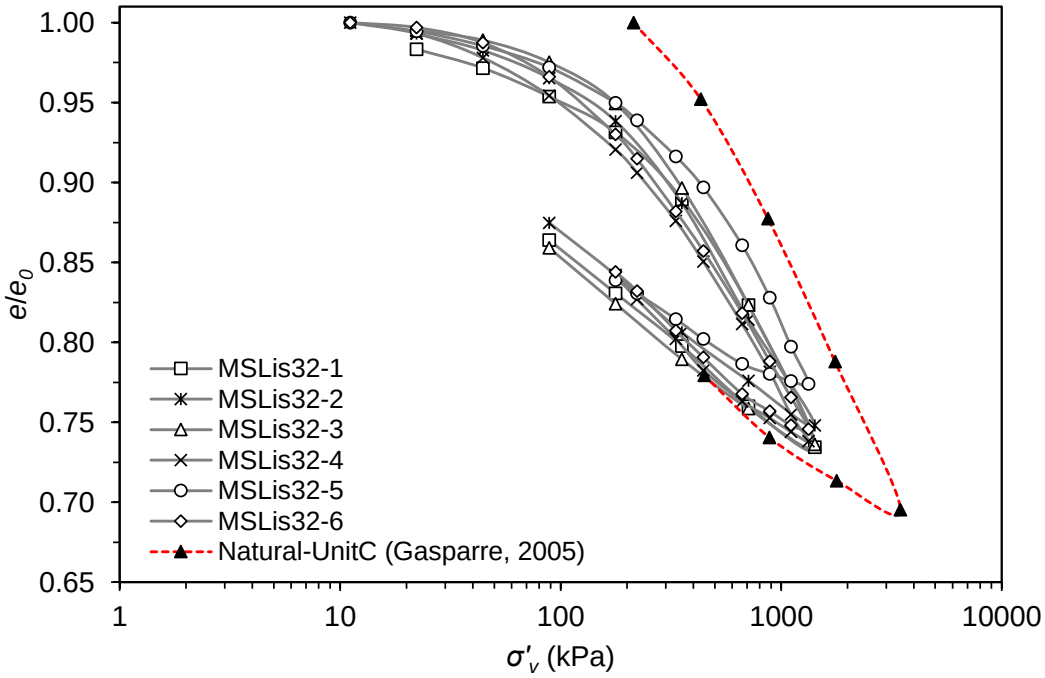

Fig. 3. Comparison of the compression curves for intact Sheppey LC and natural LC from Unit C of Heathrow T5 site

Fig. 4 presents the results of MSL compression tests carried out on reconstituted specimens. It is seen that with an increase of w_0, the compressibility of the specimens is increased. Average C_c and C_s values of respectively 0.383 and 0.125 were obtained from the compression tests on reconstituted specimens having an average initial void ratio of 0.93 and initial water content of 39%. For specimens with w_0 = 43%, the average C_c and C_s values of respectively 0.408 and 0.133 were obtained. Similar C_c values of 0.41 to 0.51 were reported by Sorensen (2006) from isotropic compression and oedometer tests on reconstituted LC from T5. Similar to intact specimens, the reconstituted compression curves of Sheppey and T5 LC were also compared. The reconstituted Sheppey specimen exhibits less compressibility in comparison with the reconstituted T5 specimen. This behaviour could be attributed to the modified PSD of the reconstituted Sheppey specimens and the presence of sand-sized aggregates that resulted in an increased resistance against compression.

Canadian Geotechnical Journal. Submitted 17 June 2018; accepted 27 June 2019.
https://doi.org/10.1139/cgj-2018-0398

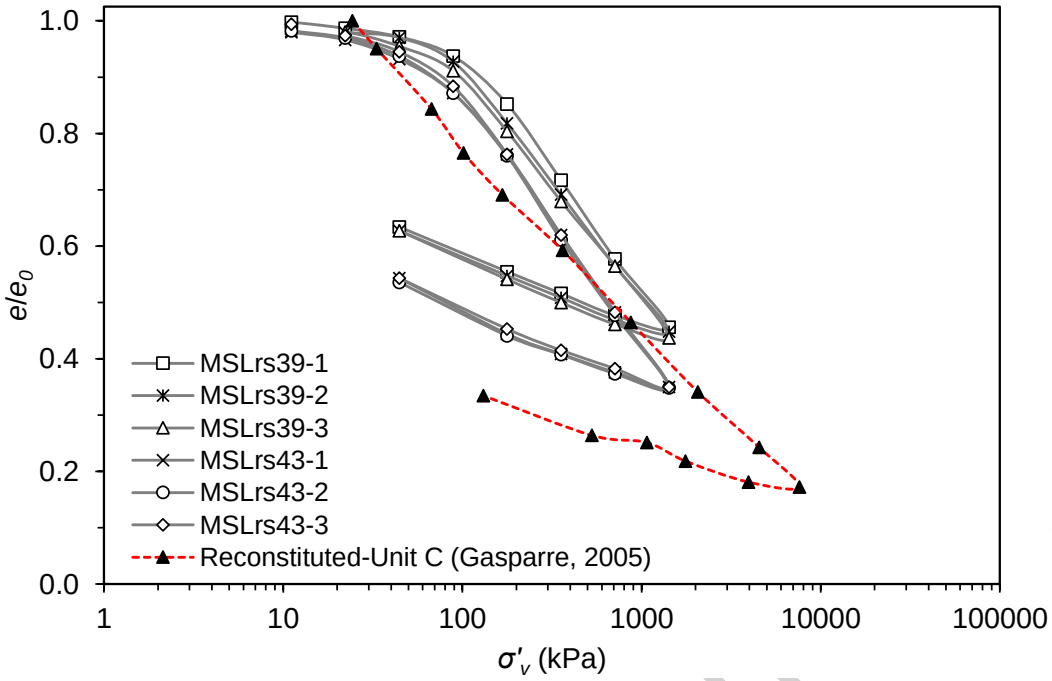

Fig. 4. Comparison of the compression curves for reconstituted Sheppey LC and natural LC from Unit C of Heathrow T5 site

To further investigate the effect of soil structure on the compressibility of Sheppey LC, a set of three MSL oedometer tests were carried out on LQU specimens. A comparison of compression curves for intact, reconstituted, and LQU specimens is shown in Fig. 5. The compression curve of the LQU specimen with partly destroyed structure lies in between the compression curves of intact and reconstituted specimens. The curve is more similar to the reconstituted compression curve, highlighting the greater influence of soil structure than the initial water content on the compressibility of stiff LC.

Canadian Geotechnical Journal. Submitted 17 June 2018; accepted 27 June 2019.
https://doi.org/10.1139/cgj-2018-0398

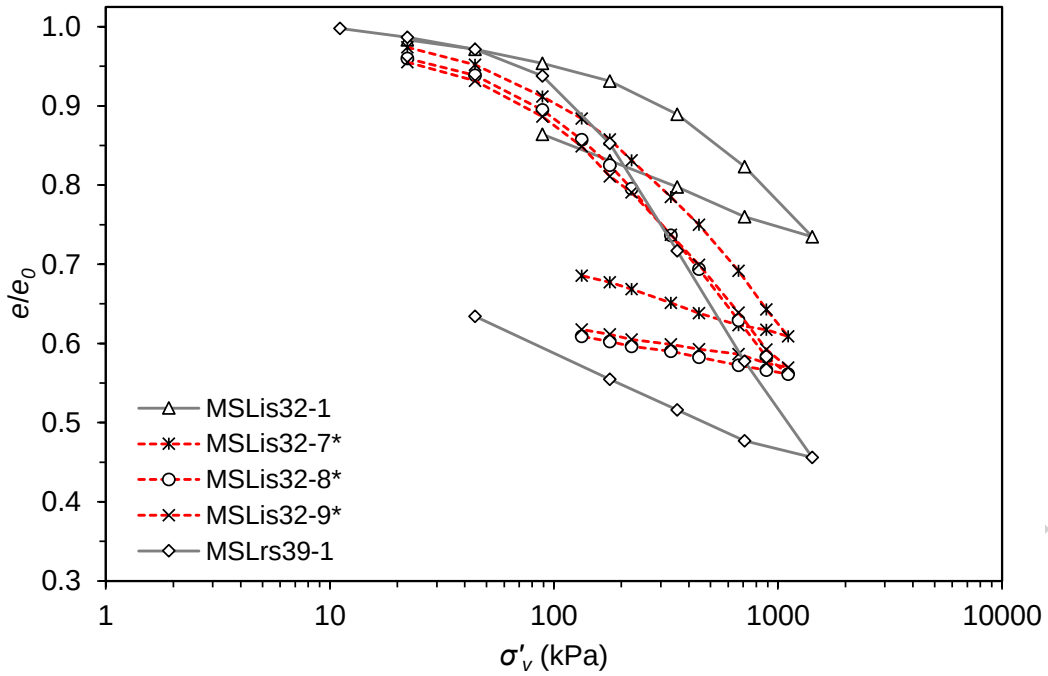

Fig. 5. Comparison of the compression curves for saturated intact, reconstituted, and LQU specimens

Fig. 6 presents the normalised compression curves for unsaturated reconstituted specimens. As it can be seen, suction influences the shape and location of the compression curves. Increase in suction level results in a decrease in overall compressibility of the specimens. Furthermore, increase in suction results in an increase in yield vertical net stress (σ_p), a phenomenon known as suction hardening (Wheeler and Sivakumar, 1995). The obtained data allows for defining the locus of the yield points in suction-net mean stress plane known as Loading-Collapse yield curve in Barcelona Basic Model (BBM) proposed by Alonso et al. (1990).

Canadian Geotechnical Journal. Submitted 17 June 2018; accepted 27 June 2019.
https://doi.org/10.1139/cgj-2018-0398

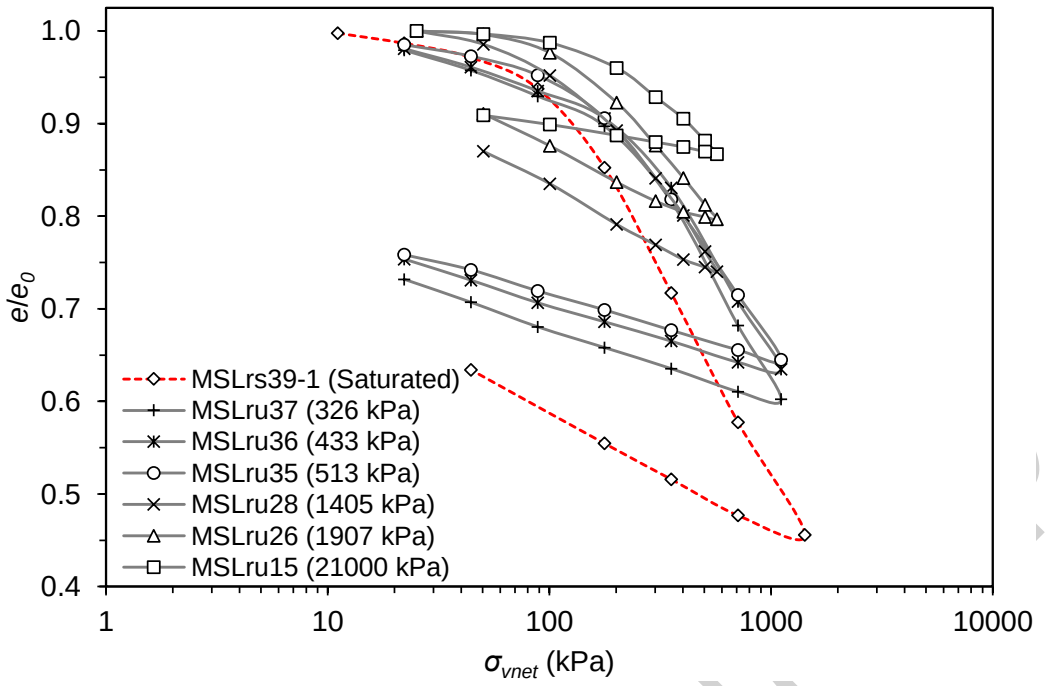

Fig. 6. Compression curves for unsaturated reconstituted specimens

Fig. 7 presents the variation of pore-water pressure (u_w) during loading and unloading stages for specimens MSLru37, MSLLru36, MSLru35 and MSLru28. Figs. 7(a) to 7(d) show an instantaneous increase in u_w (decrease in suction) followed by a gradual pressure equalisation at each loading stage. Moreover, for all loading stages, a suction state was preserved within the specimens, confirming that no water had been expelled, and hence, the condition of constant water content was recognised throughout the experiments. Similarly, instantaneous decrease in u_w (increase in suction) followed by a pressure stabilisation was observed at each unloading stage. Unlike the assumption of pore-fluid incompressibility in saturated consolidation theory, the pore-fluid, being formed of gas (typically air) and liquid (typically water), is considered compressible during consolidation of unsaturated clays. Therefore, during the course of compression, with a decrease in air volume, the S_r is increased, this is mainly due to the reduction in void ratio of the specimen. The decrease in suction observed at the end of the unsaturated MSL tests can be, therefore, explained by the increase in S_r of the specimen.

Figs. 7(e) to 7(h) present the variation of suction with vertical stress changes ($ds/d\sigma$), once equilibrium has been reached. As it can be seen on the graphs, suction is decreased during loading and then increased by unloading. For vertical stresses up to 400 kPa (200 kPa for MSLru28), a linear relationship between changes in suction and applied vertical stress was observed. Variation of suction with vertical stresses higher than 400 kPa (200 kPa for MSLru28) appears to be almost constant during both loading and unloading stages. The slopes obtained during loading were very close and varied between -0.30 and -0.34. Except for the MSLru28 specimen, the slopes obtained during unloading were also close and varied between -0.02 and -0.08. MSLru28 exhibited a higher slope in unloading (-0.86) than loading (-0.30). For natural clays, the slopes obtained during the unloading stage can be used for estimation of suction changes during sampling and release of stresses (Delage et al. 2007). Although the experiments were performed on reconstituted samples, the obtained results clearly confirmed the importance of suction and suction release, in particular in stiff clays such as LC, even though it appears that suction changes during unloading for specimens with low initial suctions (< ~500 kPa) is not significant.

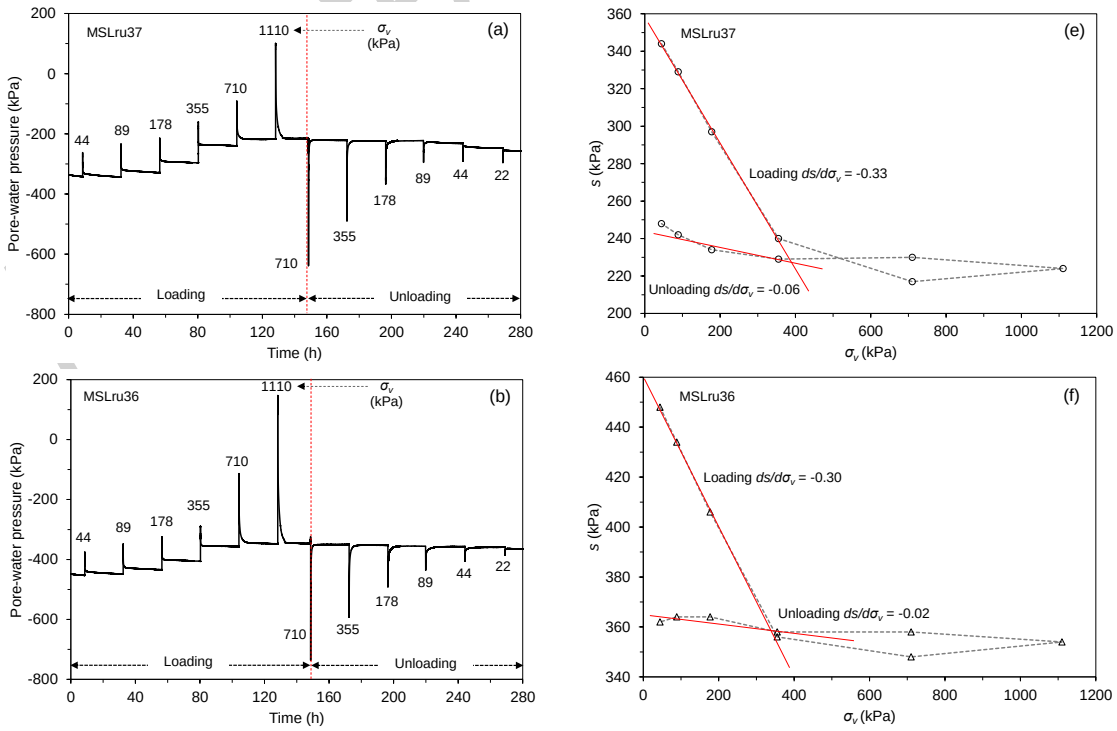

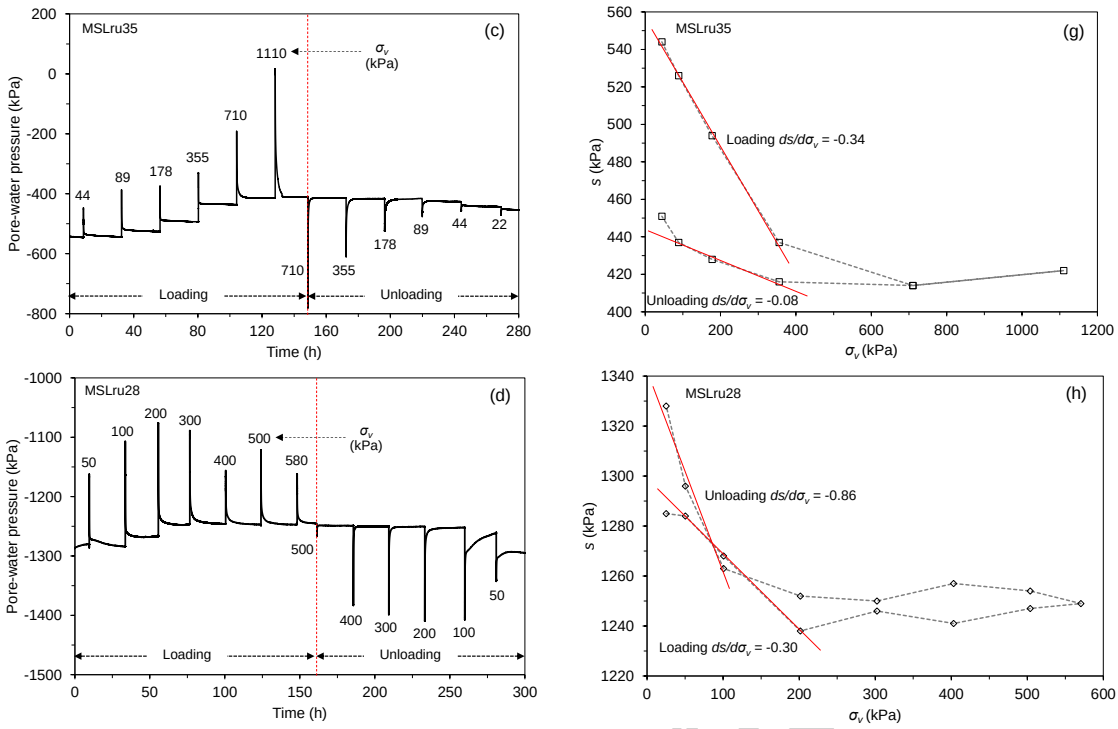

Fig. 7. Monitoring suction changes during step loading oedometer tests

Further inspection of Figs. 7(a) to 7(d) reveals a slight increase in equalised suction at the early stages of loading (e.g. at σ_v = 89 kPa) for MSLru37, MSLru36, and MSLru35 specimens. A possible reason for such observation is that under constant water content conditions, the change in pore-water pressure (Δu) is expressed as;

$$\Delta u = B \times \Delta \sigma_v + \Delta u_d \quad (2)$$

Where B is the Skempton B value ($\Delta u/\Delta \sigma_v$) and Δu_d is the excess pore-water pressure accounted for a possible dilation within the aggregates. This dilation component (Δu_d) would be negative, therefore it may subdue the overall increase in Δu caused by $\Delta \sigma_v$. Therefore, it may be expected to see an increase in suction and hence, reduction in the overall B value at the early stages of compression under undrained conditions. Evolution of B value with vertical net stress during the loading and unloading stages is shown in Fig. 8. The fact that the B value is notably high at the early stages of loading might be due the high water content of the soil paste placed on the tip of HCT to ensure intimate contact between the porous filter and surrounding soil.

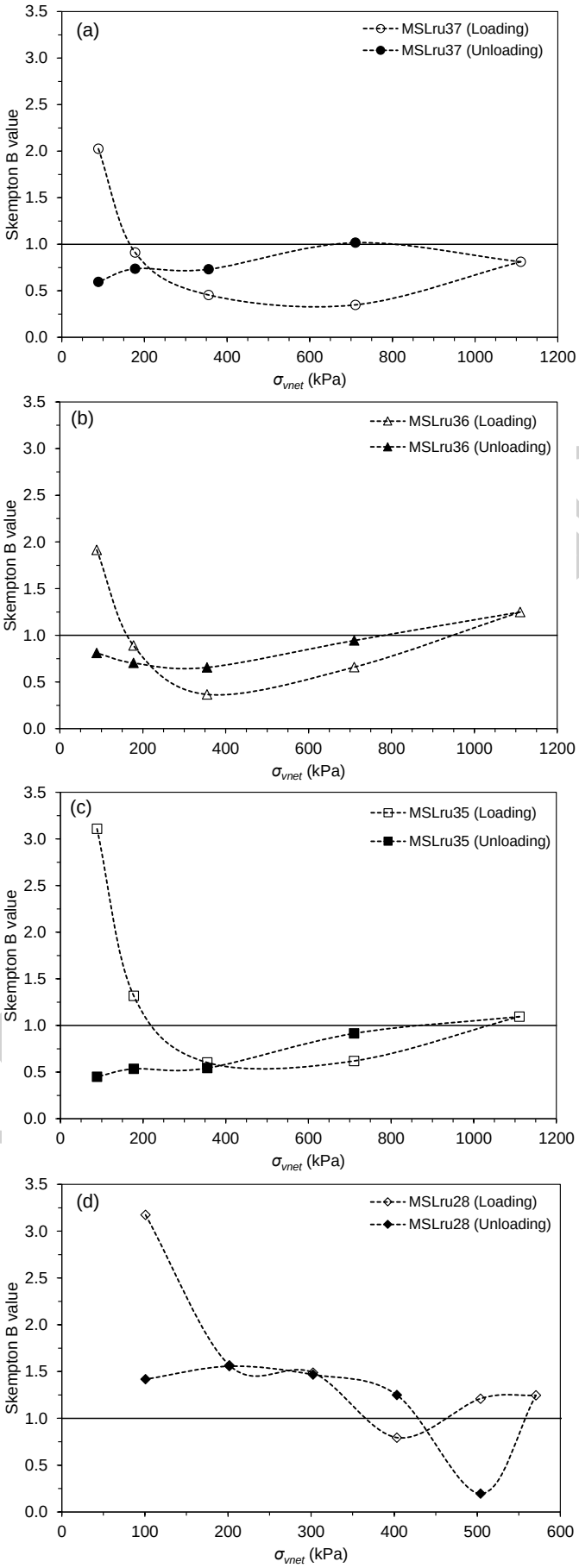

Fig. 8. Evolution of Skempton B value with vertical net stress

Stress-Dependent Response in MSL Tests

Compressibility of intact and reconstituted clays can be evaluated from the variation of the slope of compression curve with vertical effective stress (σ'_v). The slope of compression curve (m_c) at each loading increment is calculated as $\Delta e/\Delta \log \sigma'_v$. The saturated yield vertical net stress (σ'_p) was determined as the intersection of the best fitted lines to the pseudo-elastic and plastic sections of the compression curve. For $\sigma'_v < \sigma'_p$, the calculated values represent the slope of the reloading line (i.e. C_r), and for $\sigma'_v > \sigma'_p$, the calculated values represent the slope of normal compression line (i.e. C_c). Fig. 9 presents the relationship between m_c and normalised stress σ'_v/σ'_p for saturated intact, reconstituted, and LQU specimens. As it can be seen, change in the loading pattern (dotted lines) does not have a significant influence on the C_r and C_c values for intact specimens. Prior to the yield stress, the C_r values increase slightly. Following σ'_p, the values of C_c increase gradually until reaching a peak value around (8-10) σ'_p, after which, a gradual decrease in compressibility is observed. Unlike soft clays that exhibit a sudden increase of C_c in post yield region due to structural collapse (see for example Mataic et al. 2016), the process of destructuration in stiff LC appears to be continuous and follows an almost linear trend until reaching the peak value. In soft clays the peak value falls in a range of (2-3) σ'_p (e.g. Karstunen and Yin 2010; Mataic et al. 2016), whereas for stiff LC this range is observed to extend to (8-10) σ'_p (see Fig. 9). Similar to intact specimens, the slope of reloading line for reconstituted specimens increases slightly prior to σ'_p. Increase in slope of reloading line for specimens with w_0 = 43% is reasonably higher than the specimens with w_0 = 39% given the higher water content that results in higher compressibility. The slope of compression curve in normal consolidation (NC) region increases dramatically to a peak value at stress levels between (3-4) σ'_p, at which it starts to decrease slowly. In soft clays, higher m_c values for intact specimens is typically observed in comparison with the reconstituted specimens, mainly due to the destructuration phenomenon that results in dramatic increase of C_c values in post yield region. However, as explained earlier, in stiff LC, degradation of inter-particle

bonds (destructuration) does not occur suddenly and typically takes place gradually with increase in stress level. In overconsolidated (OC) region, the C_r values for LQU specimens increase at the same rate as the reconstituted specimens. However, in post yield region, the rate of increase in C_c for LQU specimens is lower than that of reconstituted specimens, this is in part, due to the lower w_0 and the presence of inter-particle bonds that result in reduction of compressibility. The maximum value of C_c for LQU specimens occurs in a range of (6-8) σ'_p.

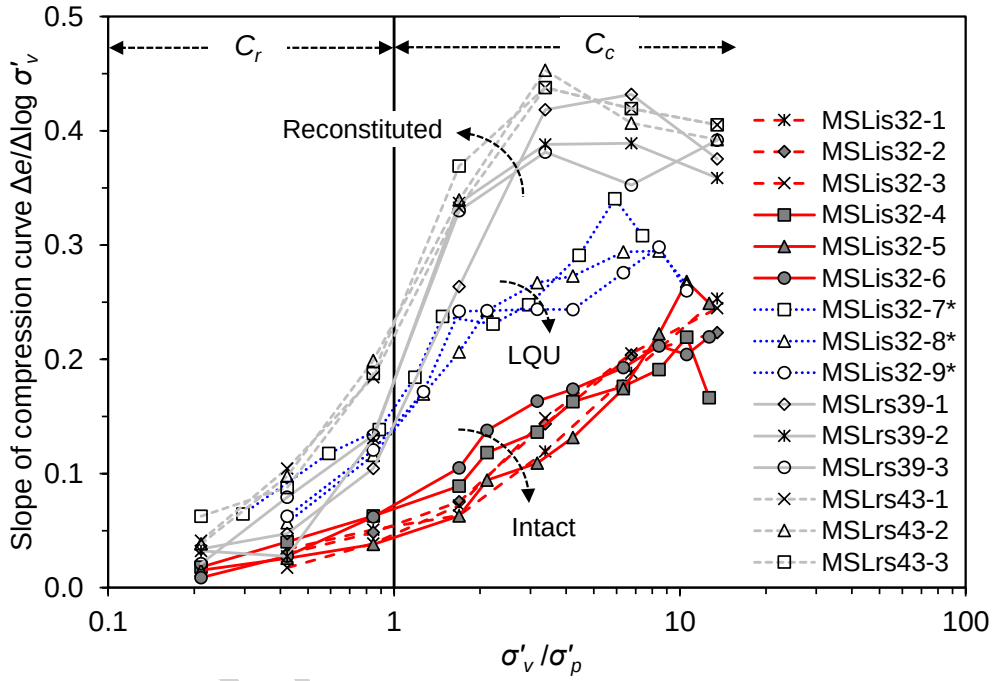

Fig. 9. Stress-dependency of the slope of compression curve for saturated intact, reconstituted, and LQU specimens

Fig. 10 presents variation of the $C_{\alpha e}$ with normalised stress σ'_v/σ'_p for intact, reconstituted, and LQU specimens. It is observed that for doubling vertical stress method (dotted lines), $C_{\alpha e}$ increases gradually with stress level up to (3-4) σ'_p, at which it starts to increase dramatically to a peak value at stress levels in a range of (6-7) σ'_p. This behaviour can be attributed to the structural damage to the specimen during sudden loading at high stress levels. After the peak value, $C_{\alpha e}$ decreases dramatically. For specimens that the vertical stresses were applied in an unconventional way (continuous lines) following the pattern described in Table 2, it is observed that $C_{\alpha e}$ increases

gradually with stress level up to (8-11) σ'_p, at which it starts to decrease. This unconventional loading method, therefore, appears to produce more reliable results although it involves more loading stages and hence, requires more time to complete. The maximum value of $C_{\alpha e}$ falls approximately in the range of 0.007 – 0.008 and 0.005 – 0.006 respectively for conventionally and unconventionally loaded intact specimens. For reconstituted specimens with w_0 = 39%, $C_{\alpha e}$ increases slowly at stress levels prior to σ'_p. For stresses beyond yield stress, $C_{\alpha e}$ increases at a higher rate until reaching a peak value at stress levels in a range of (6-7) σ'_p at which it starts to decrease. For specimens with higher initial water content (w_0 = 43%), variation of $C_{\alpha e}$ with normalised stress is slightly different, with $C_{\alpha e}$ increasing dramatically in OC region and then increasing gradually in NC region to a peak value at stress levels in a range of (3-4) σ'_p where a gradual reduction of $C_{\alpha e}$ values is observed. The maximum value of $C_{\alpha e}$ falls approximately in the range of 0.012 – 0.013 for all tested reconstituted specimens. This range is comparable with the average value of $C_{\alpha e}$ = 0.016 reported by Sorensen (2006) for reconstituted T5 LC.

Unlike natural soft clays which typically exhibit higher creep than their corresponding reconstituted specimens, stiff LC exhibits significantly less creep in comparison with the corresponding reconstituted specimens. This, on the one hand, can be attributed to the more compact nature of stiff clays (low initial void ratio) that results in reduced particles freedom for rearrangement under sustained σ'_v, and on the other hand, to the low w_0 of the intact specimens and presence of localised unsaturated pockets with sustainable water menisci developed at inter-particle contacts preventing orientation and rearrangement of particles into a more packed state. In soft clays, the $C_{\alpha e}$ values for intact specimens essentially converge with intrinsic $C_{\alpha e}$ of the reconstituted specimens at high stress levels associated with the completely destroyed inter-particle bonds and rearranged fabric (Mataic et al. 2016). Indeed, much higher stress levels are required to observe such behaviour for stiff clays. For LQU specimens, it is observed that $C_{\alpha e}$ increases gradually with stress level up to (4-5) σ'_p, at which it starts to decrease. The response of

325 LQU specimens is more similar to that of reconstituted ones, highlighting the effect of soil
326 structure on creep strains.

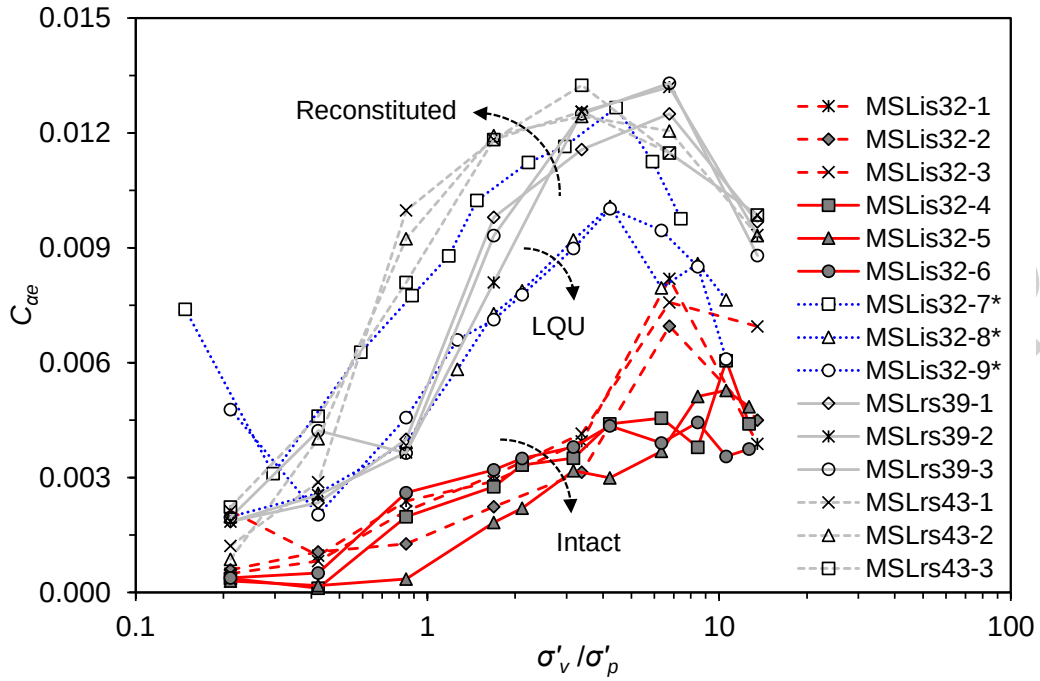

327
328 **Fig. 10.** Stress-dependency of $C_{\alpha e}$ for intact, reconstituted, and LQU specimens

329 The ratio of $\alpha = C_{\alpha e}/C_c$ in clays has been the subject of numerous studies in the past. Although
330 early researchers such as Mesri and Godlewski (1977) and Mesri and Castro (1987) proposed
331 constant values for α, recent experimental studies (e.g. Yin et al. 2011; Mataic et al. 2016) have
332 demonstrated stress-dependency of α for soft clays. In order to examine the applicability of either
333 of these two hypotheses for stiff Sheppey LC, the ratio α was investigated. Fig. 11 presents
334 variation of $C_{\alpha e}/m_c$ ratio with normalised stress σ'_v/σ'_p for saturated intact, reconstituted, and LQU
335 specimens. Unlike natural soft clays that exhibit a sudden increase to a peak value in post yield
336 region due to destructuration phenomenon (Mesri and Castro 1987; Karstunen and Yin 2010;
337 Mataic et al. 2016), variation of $C_{\alpha e}/m_c$ ratio with normalised stress for intact specimens does not
338 present such trends. At lower stress levels (i.e. OC region), the $C_{\alpha e}/C_r$ ratio is considerably
339 scattered. In NC region, the $C_{\alpha e}/C_c$ ratio decreases gradually with stress level. The values of α fall
340 approximately in a range of 0.015 – 0.045. Moreover, the values of α for conventionally loaded

specimens are generally greater than those of unconventionally loaded specimens (dotted lines). The less scattered values of α for unconventionally loaded specimens in post yield region can further approve the suitability of this loading method for investigating interrelation of compression and creep indices in stiff clays. Similar to intact specimens, the $C_{\alpha e}/C_r$ ratio for reconstituted specimens is considerably scattered at lower stress levels (i.e. OC region). However, in NC region, the $C_{\alpha e}/C_c$ values are less scattered and decrease gradually to finally converge at the constant average value of 0.024. Moreover, the values of α in post yield region are in general smaller for intact specimens than reconstituted ones given lower C_c and $C_{\alpha e}$ values observed for intact specimens (see Figs. 9 and 10). In soft clays, the $C_{\alpha e}/C_c$ values essentially converge at a constant value corresponding to that of the reconstituted specimens. This is justified based on the principle that at high stress levels, all inter-particle bonds are destroyed and the post yield compression curve of a natural clay merges with the intrinsic compression line (ICL) associated with the corresponding reconstituted specimen. In soft clays, convergence of $C_{\alpha e}/C_c$ values for intact and reconstituted specimens may occur at stress levels in a range of (10-20) σ'_p due to the soft nature and high degree of destructuration in these materials. However, a much higher stress level may be required for degradation of inter-particle bonds in stiff clays such as LC. Applying such high stresses may not be typically possible using the conventional dead-weight loading method in oedometer apparatuses. Inspection of the results for LQU specimens reveals that, except for the MSLis32-7* specimen, the ratio of α for LQU specimens exhibits a peak value at stress levels in a range of (4-5) σ'_p, at which it starts to decrease towards the values of α ratio of the reconstituted specimens. In conclusion, it is clear that the $C_{\alpha e}/C_c$ ratio is stress-dependent and varies with the effective stresses. Therefore, the hypothesis of constant $C_{\alpha e}/C_c$ ratio is not applicable for the tested material.

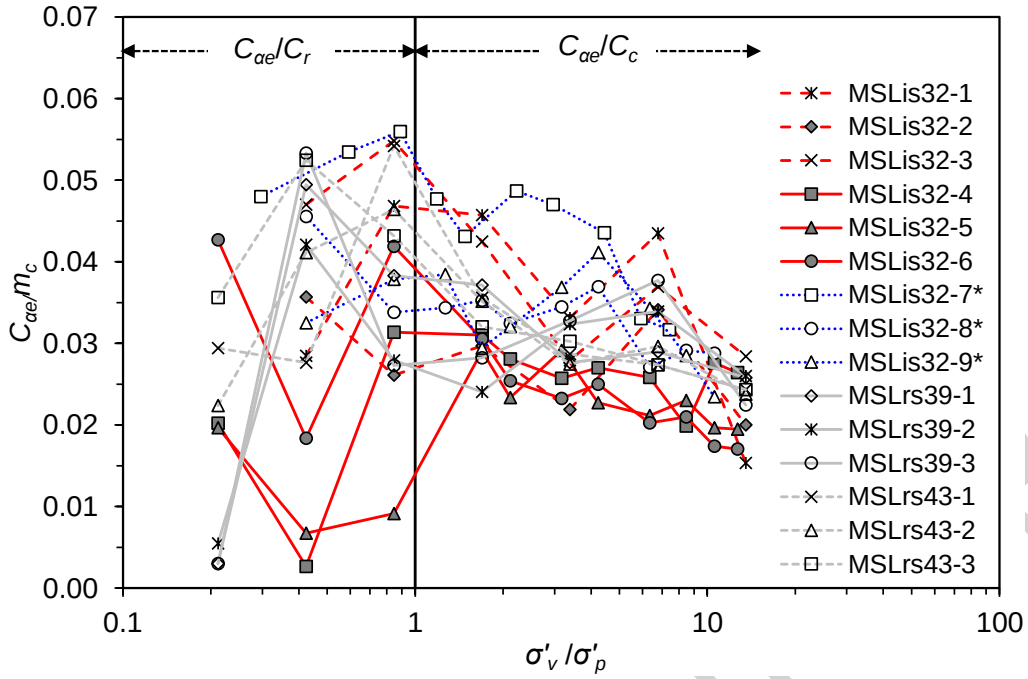

Fig. 11. Stress-dependency of C_{ae}/C_c for intact, reconstituted, and LQU specimens

Suction-Dependent Response in MSL Tests

Fig. 12 presents the relationship between the slope of unsaturated compression curve (m'_c = $\Delta e/\Delta \log \sigma_{vnet}$) and vertical net stress (σ_{vnet}) for unsaturated reconstituted specimens. Similar to saturated reconstituted specimens (see Fig. 9), the slope of compression curves, calculated for each load increment, exhibits stress-dependency and increases with increase in σ_{vnet}. However, unlike the saturated specimens, a peak value, after which the m'_c is decreased, is not apparent. Moreover, it is clearly shown that increase in suction results in decrease of the m'_c values. To further investigate this phenomenon, the values of C_s and C_c for each test were plotted against the initial suction of the specimen (Fig. 13). It is clearly observed that the C_c values decrease with increase in suction. The C_s values also decrease with increase of suction and follow an approximately linear trend. The latter observation contradicts with the statement of Sivakumar (1993) that the gradient of swelling lines are almost independent of suction level. The former observation also contradicts with the results of suction-controlled oedometer tests on compacted LC, performed by Monroy et al. (2008), who reported an increase in C_c values with increase in soil suction. The reason behind

such contradiction can be attributed to the sample preparation method and the initial conditions of the test specimens. Monroy et al. (2008) prepared the samples by static compaction to an initial suction of 1000 kPa, and then decreased the suction by hydrating the samples to different equilibrium suctions (zero, 120, and 405 kPa). Therefore, the observed differences in compressibility responses can be explained, in one hand, by the differences in mechanical response of compacted and reconstituted samples, and in other hand, by the initial hydraulic states of the two samples positioned respectively on the main drying (reconstituted) and main wetting (compacted) curves of the SWRC.

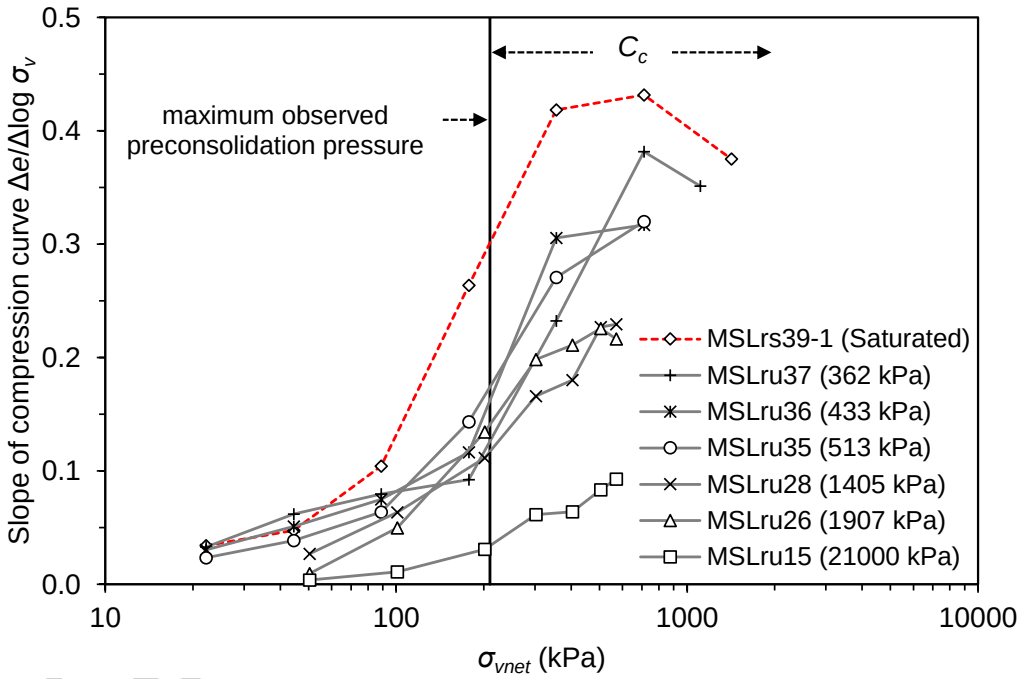

Fig. 12. Suction- and stress-dependency of the slope of compression curve for unsaturated reconstituted specimens

Canadian Geotechnical Journal. Submitted 17 June 2018; accepted 27 June 2019.
https://doi.org/10.1139/cgj-2018-0398

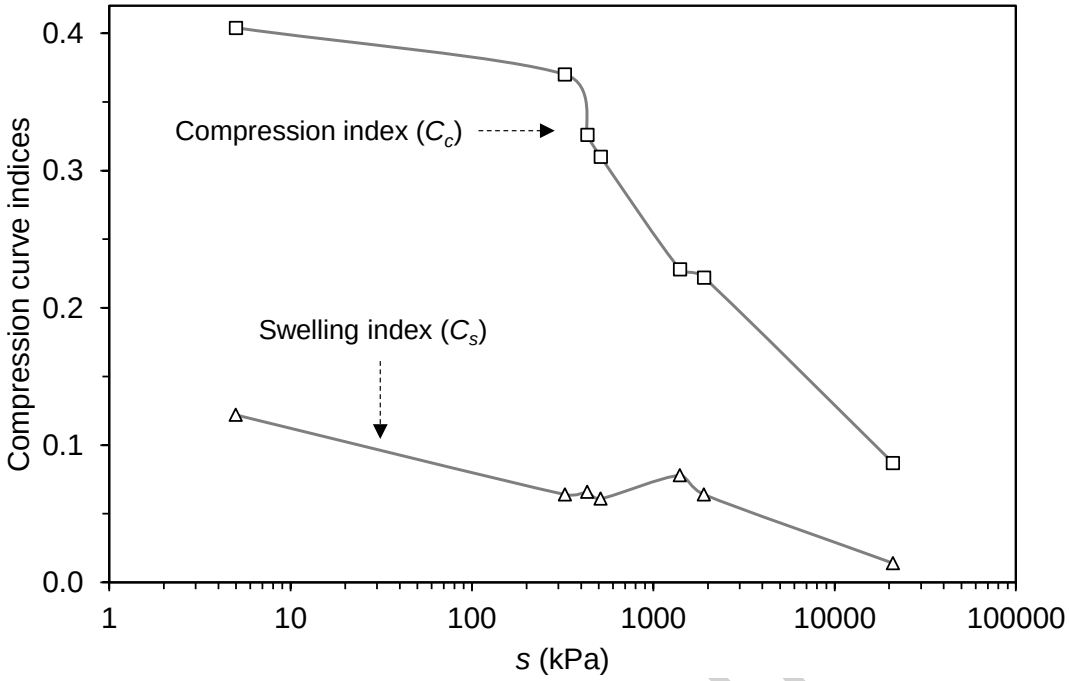

Fig. 13. Variation of C_c and C_s with suction for unsaturated reconstituted specimens

The compression index as a function of suction has been the subject of a long-term dispute among the researchers. Different approaches, as discussed in Zhou et al. (2012), have been proposed to overcome the problems associated with assuming C_c as a function of suction. Among which, the assumption of C_c as a function of S_r appears to be a more logical approach which also produces a better match to the experimental data when used in constitutive models (Zhou et al. 2012). This approach implies that C_c increases with increase in S_r. In other words, it is possible to saturate an unsaturated soil by compressing it under constant suction. In fact, in constant suction compression, increase in S_r as a result of reduction in void ratio, can increase the compressibility of the soil due to the stress-induced collapse of macro-pores (Zhou et al. 2012). Based on this approach, increase of C_c is small at low stresses, and becomes larger at intermediate stress levels until finally equalises the C_c value corresponding to the saturated condition. This behaviour is clearly shown in Fig. 12. The only difference is that the C_c values of unsaturated specimens do not essentially converge with the values of their saturated condition. Higher applied total stresses might be required to observe such convergences. Moreover, as shown in Fig. 7, in drained compression tests carried out here, suction evolves throughout the experiment and ends up with a lower value than the s_0 at the start

of the test. Therefore, the conditions of constant suction tests, typical of suction-controlled oedometer tests, are not met here. Essentially, for the material tested here, it can be concluded that the slope of compression curve decreases with increase of soil suction.

Fig. 14 presents variation of the $C_{\alpha e}$ with vertical net stress (σ_{vnet}) for unsaturated reconstituted specimens. Similar to saturated reconstituted specimens (see Fig. 10), the $C_{\alpha e}$, calculated for each load increment, exhibits stress-dependency and increases with increase in σ_{vnet}. However, unlike the saturated specimens, a peak value, after which the $C_{\alpha e}$ is decreased, is not apparent. In a rough estimation, for specimens with s_0 of 362, 1405, 1907, and 21000 kPa, the maximum value of creep index appears to occur at 710, 500, 500, and 400 kPa vertical total stress respectively. Furthermore, increase of $C_{\alpha e}$ is small at low stress levels (< 200 kPa), and becomes larger at higher stress levels. Moreover, it is clearly observed that increase in suction results in a decrease of the $C_{\alpha e}$ values. With development of partial saturation state in the specimen during drying, the u_w becomes negative at the back of the generated water menisci at the inter-particle contacts, applying tensile pressure to the soil grains. The additional attractive forces exerted from the water menisci and contractile skin, contribute to the reduction of particles' freedom for rearrangement under sustained effective stress. The rate and magnitude of volumetric creep strains (ε_v^{cr}) are, therefore, decreased with the increase in soil suction.

Canadian Geotechnical Journal. Submitted 17 June 2018; accepted 27 June 2019.
https://doi.org/10.1139/cgj-2018-0398

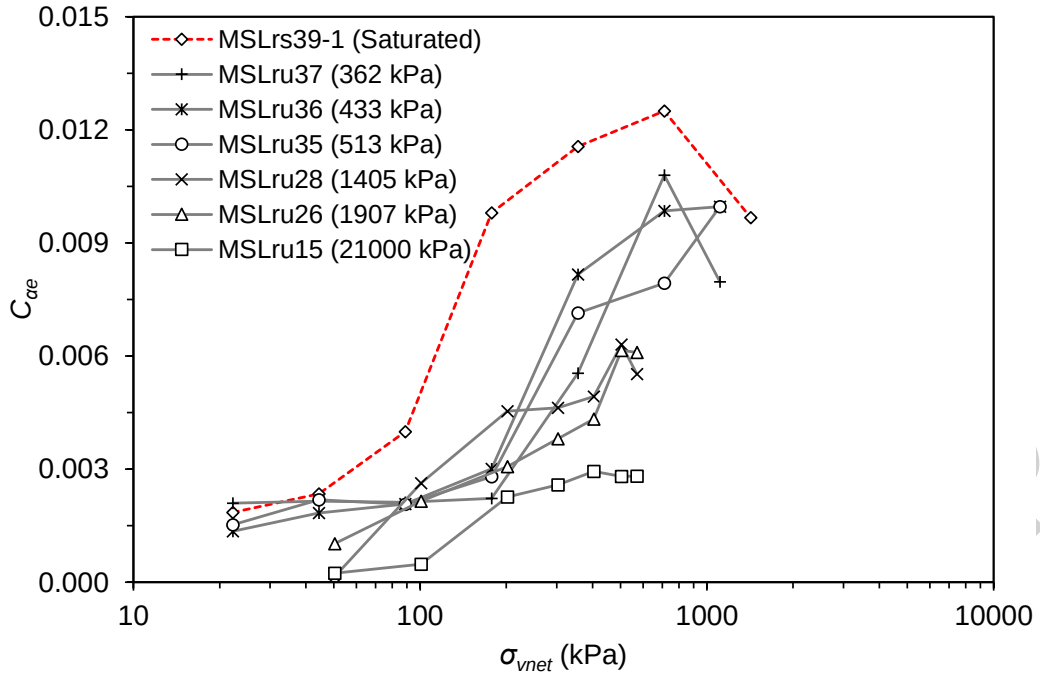

Fig. 14. Suction- and stress-dependency of $C_{\alpha e}$ for unsaturated reconstituted specimens

Fig. 15 presents the variation of $C_{\alpha e}/m'_c$ ratio with vertical net stress for unsaturated reconstituted specimens. At low stress levels (< 200 kPa), the values of $C_{\alpha e}/m'_c$ decrease with increase in σ_{vnet}. However, at higher stress levels, the values of $C_{\alpha e}/m'_c$ are scattered and do not follow a clear trend. In a rough estimation, the values of $\alpha = C_{\alpha e}/C_c$ could approximately be considered constant with increase in stress level. Excluding the MSLru15 specimen, the values of α obtained for unsaturated conditions appear to fall within a range of 0.023 – 0.030. Note that in saturated conditions, the values of α decrease gradually to finally converge at a constant value of 0.024, whereas in unsaturated conditions a clear trend and/or convergence is not observed.

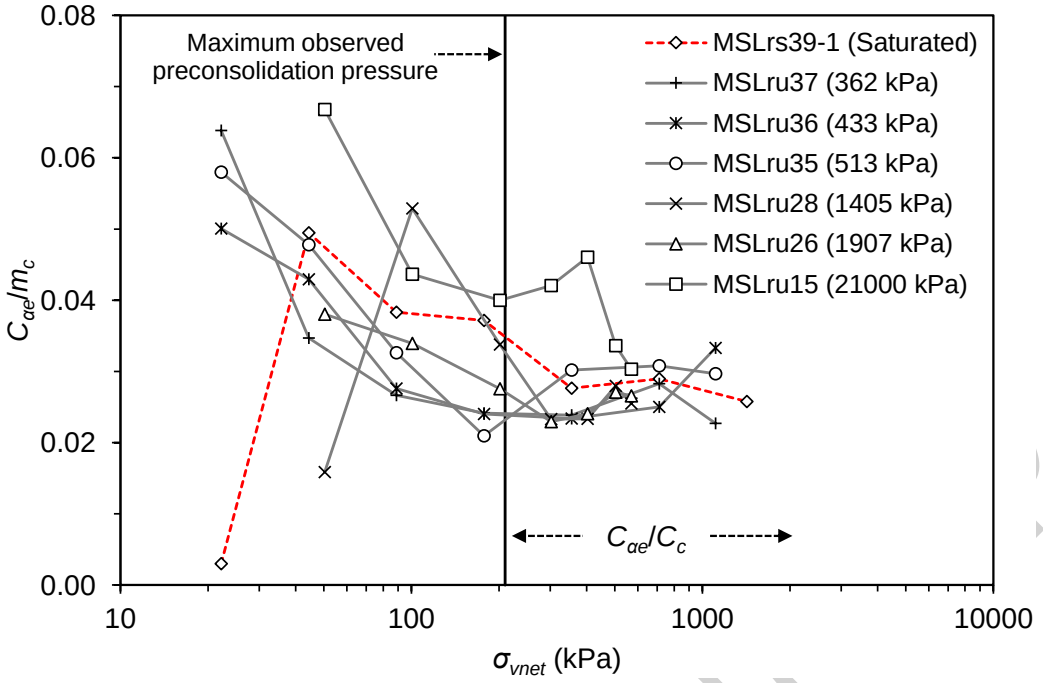

436

437 **Fig. 15.** Suction- and stress-dependency of the α ratio for unsaturated reconstituted specimens

438 ***Evaluation of α Ratio for Sheppey London Clay***

439 Table 4 summarises the stress ranges at which the maximum values of C_c, $C_{\alpha e}$, and α occur for
440 both intact and reconstituted specimens. The range and average values of α ratio obtained from
441 different sets of experiments are also presented. The results indicate that for conventionally loaded
442 intact specimens as well as reconstituted specimens with w_0 = 0.39, the maximum values of C_c
443 and $C_{\alpha e}$ do not occur at the same stress level. However, for unconventionally loaded intact
444 specimens as well as reconstituted specimens with w_0 = 0.43, C_c and $C_{\alpha e}$ reach the peak value at
445 the same stress levels synchronously. The latter finding is in contradiction with the limited
446 available observations reported in the literature for soft clays (see Mataic et al. 2016). The
447 maximum values of α occur at stress levels in a range of (1-2) σ'_p, for both intact and reconstituted
448 specimens. For unsaturated specimens, a peak value for C_c, $C_{\alpha e}$, and α was not apparent. For
449 saturated intact specimens, the range of α values varies significantly. For conventionally loaded
450 intact specimens, an average α value of 0.03 ± 0.02 can be approximated. However, for
451 unconventionally loaded intact specimens, a lower approximate average α value of 0.02 ± 0.01 is

obtained. According to the classification criterion defined by Mesri et al. (1994), Sheppey London Clay lies in the zone of shale or mudstone whose α value ranges from 0.02 to 0.04. For saturated and unsaturated reconstituted specimens, the ratio $C_{\alpha e}/C_c$ lies in a similar range of 0.023 – 0.037. Accordingly, an average value of 0.03 ± 0.01 can be approximated for the α ratio of saturated and unsaturated reconstituted specimens. The values of α for saturated LQU specimens fall in a range of 0.023 – 0.048, with the lower band value being equal to that of reconstituted specimens, and the upper band value, being similar to that of intact specimens.

Stress- and Suction-Dependent Response in SSL Tests

Test results in this section are presented in plots of normalised void ratio e/e_p versus logarithm of time, where e_p is the void ratio obtained 24 hours after the end of loading. The decision of considering the results obtained after a period of 24 hours was made so as to ensure full dissipation of u_{exc}, and also to allow for comparison between the results and define a criterion applicable to all experiments. Similar approach was considered by Cui et al. (2009) for investigating time-dependent behaviour of stiff Boom Clay.

Fig. 16 compares variation of the normalised void ratio e/e_p with logarithm of time for intact and reconstituted specimens at different stress levels. For all specimens, higher volume changes were observed with increase in σ_{vm}, indicating the stress-dependency of creep strains. The rate of change in void ratio for all specimens was higher during the first 10 days of sustained loading, after which it started to decrease. For intact and reconstituted specimens, the observed behaviour corresponds to primary creep stage characterised as increasing creep strains at a decreasing strain-rate. Furthermore, the creep rate and magnitude appears to be, in general, lower for intact specimens than the reconstituted ones, this being, in part, due to the low w_0 of the intact specimens. Soil structure, i.e. fabric anisotropy and inter-particle bonding, also plays a significant role in controlling deformations. The process of destructuration during single-stage loading, and whether

476 the inter-particle bonds were fully or partly destroyed, is not, however, clearly identified.
477 Moreover, at the same stress level, the rate and magnitude of change in void ratio for reconstituted
478 specimens with higher initial water contents (w_0 = 0.43) were found to be higher. In the absence
479 of inter-particle bonds, the water content of the specimens appears to control the rate and
480 magnitude of creep strains.

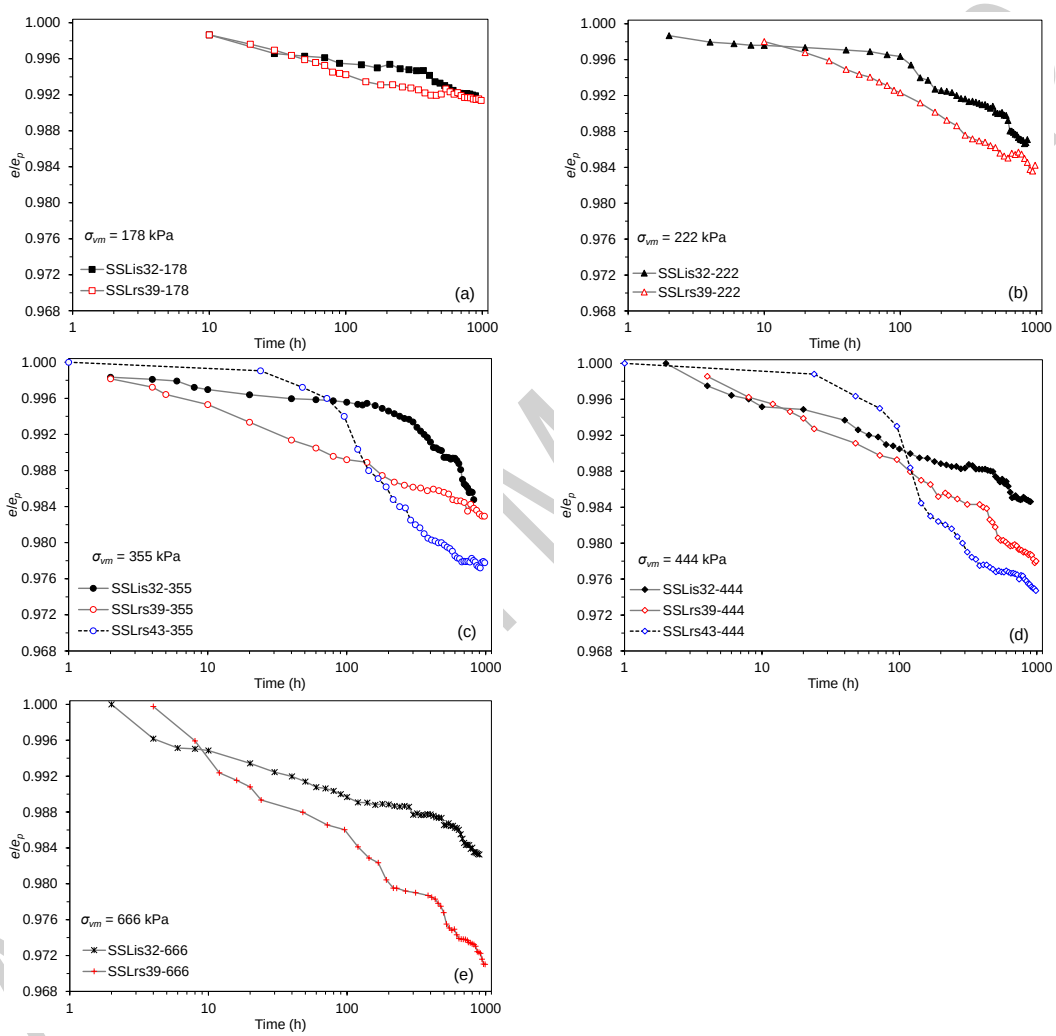

481 **Fig. 16.** SSL creep test results on intact and reconstituted specimens at stress levels of: (a) 178 kPa; (b)
482 222 kPa; (c) 355 kPa; (d) 444 kPa; (e) 666 kPa

483 Graphs of Fig. 17 present the variation of normalised void ratio e/e_p with logarithm of time for
484 specimens having different initial water contents (and therefore different suctions), and subjected
485 to similar vertical stresses. It is clearly observed that at the same vertical stress level, decrease in

w_0 (or increase in s_0) results in a decrease in the rate and magnitude of ε_v^{cr}. Unlike saturated soils, the water phase in partially-saturated soils is discontinuous. The generated water menisci between the soil particles hold the grains together and the soil particles are held together by the tensile forces at the solid-water interface. During creep under constant effective stress, the under-tension water menisci resist against rearrangement and orientation of the clay particles.

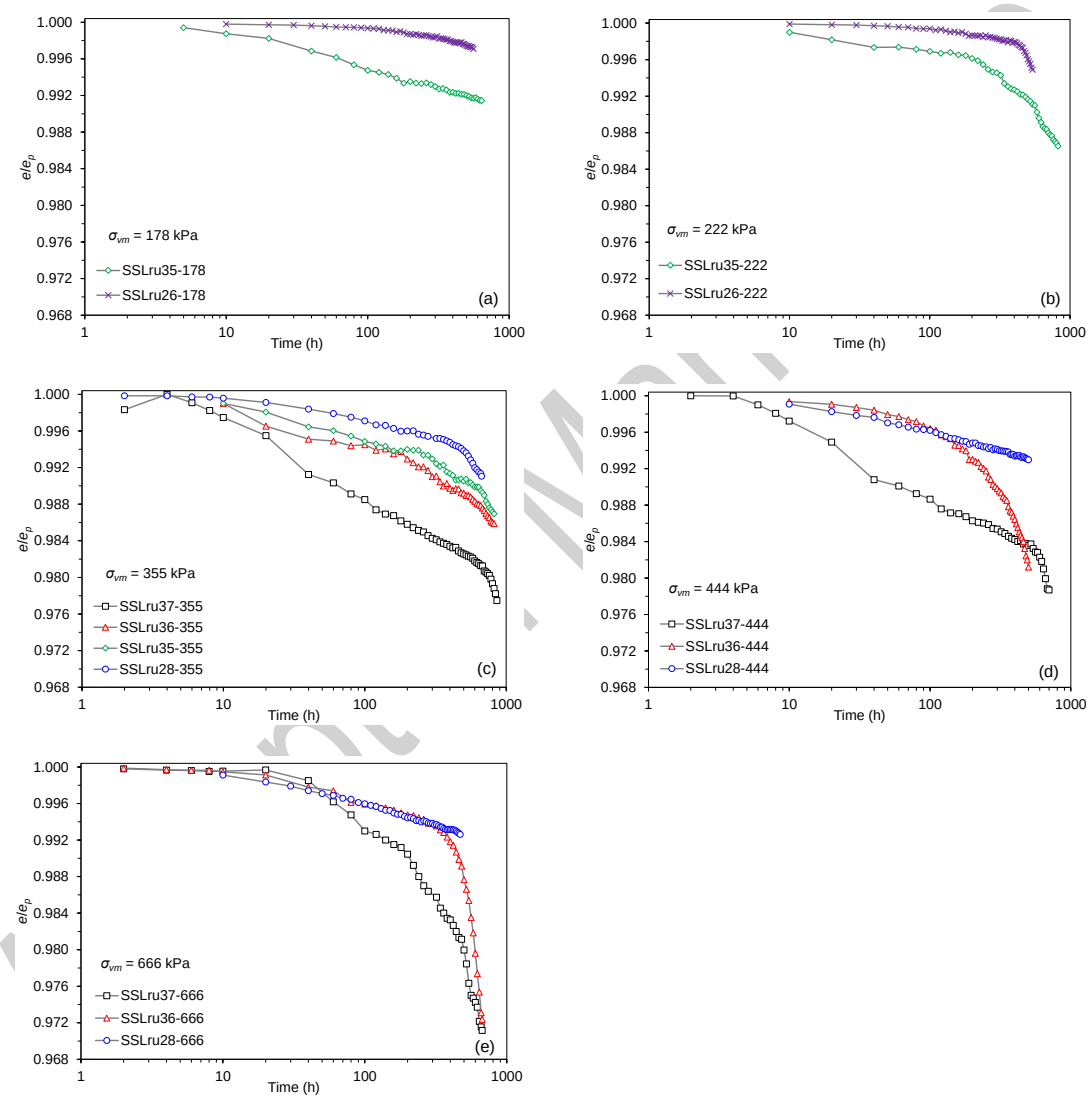

Fig. 17. SSL creep test results on unsaturated reconstituted specimens at stress levels of: (a) 178 kPa; (b) 222 kPa; (c) 355 kPa; (d) 444 kPa; (e) 666 kPa

Similar to saturated conditions (Fig. 16), creep behaviour in unsaturated conditions appears to be stress-dependent. However, effect of increase in σ_{vm} is more pronounced during the final stages of

Canadian Geotechnical Journal. Submitted 17 June 2018; accepted 27 June 2019.
https://doi.org/10.1139/cgj-2018-0398

the unsaturated tests. For specimens SLLru28-444 and SLLru28-355 with s_0 = 1405 kPa, the volume change response appears to be fairly similar, indicating the predominant effect of soil suction in controlling creep deformations. Similar behaviour is also observed for SLLru26-222 and SLLru26-178 specimens with s_0 = 1907 kPa, further supporting this hypothesis. The predominant effect of suction is not, however, apparent for specimens with lower initial suctions. Similar to MSL tests, an instantaneous increase in u_w (decrease in suction) followed by a gradual pressure equalisation at each loading stage was observed. Moreover, for all loading stages, a suction state was preserved within the specimens, confirming that no water was expelled, and hence, the condition of constant water content was recognised throughout the loading stage. Fig. 18 presents the results of monitoring suction evolutions during the creep stage of the tests. It is observed that suction is decreased with time for all of the test specimens. In fact, with increase in creep strains at constant water content, total volume is decreased resulting in an increase in the S_r, which in turn, leads to a decrease in soil suction. This is, however, a possible mechanism, and the observed decrease in suction might be due to other factors influencing the HCTs measurements. However, if this is the case, keeping the soil suction constant during a constant suction creep test may not be ideal, as this may require a change (reduction) in S_r of the specimen, and hence, artificially development of creep strains.

Canadian Geotechnical Journal. Submitted 17 June 2018; accepted 27 June 2019.
https://doi.org/10.1139/cgj-2018-0398

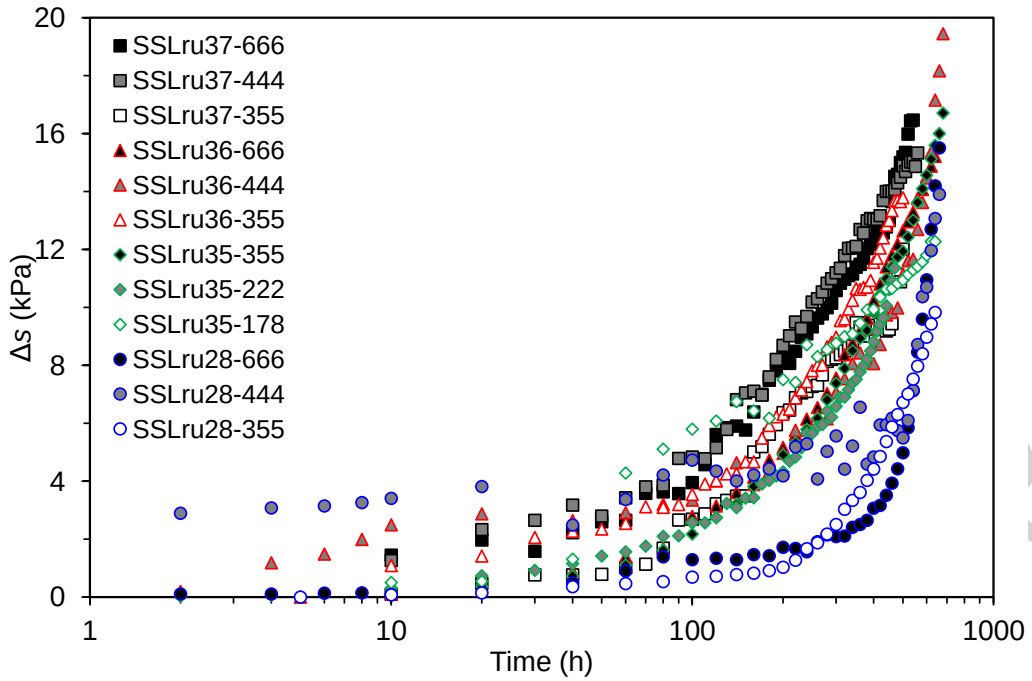

Fig. 18. Monitoring suction changes during creep stage of SSL oedometer tests

Conclusions

Results of a set of MSL and SSL oedometer tests performed on Sheppey London Clay specimens under different conditions of saturated intact, saturated reconstituted, and unsaturated reconstituted were presented. The following conclusions can be drawn;

- The change in loading pattern, which was aimed at reducing the effects of sudden loading and subsequent damages to the soil structure during MSL tests, does not have a notable influence on the obtained compression curves and the C_r and C_c values for intact specimens; however, it leads to lower $C_{\alpha e}/C_c$ values than the conventionally loaded specimens.
- Unlike soft clays that exhibit a sudden increase of C_c in the post yield region due to structural collapse, the process of destructuration in stiff LC appears to be continuous and follows an almost linear trend.
- Unlike natural soft clays which typically exhibit higher creep than their corresponding reconstituted specimens, stiff LC exhibits significantly less creep in comparison with the corresponding reconstituted specimens. This, on the one hand, can be attributed to the more

compact nature of stiff clays (low e_0), and on the other hand, to the low w_0 of the intact specimens.

- Generally, for Sheppey LC, increase in suction results in a decrease in the slope of compression curve (m'_c) and the $C_{\alpha e}$ values, and an increase in σ_p.
- According to the classification criterion defined by Mesri et al. (1994), Sheppey LC is categorised as shale or mudstone whose α value ranges from 0.02 to 0.04. The $\alpha = C_{\alpha e}/C_c$ ratio for Sheppey LC is stress- and suction-dependent, and therefore cannot be considered as a constant value. However, as a rough estimation, an average value of 0.03 ± 0.01 can be approximated for the α ratio of saturated and unsaturated reconstituted specimens.
- During SSL tests, at the same vertical stress level, decrease in w_0 (or increase in s_0) results in a decrease in the rate and magnitude of ε_v^{cr}. Moreover, at the same s_0, increase in applied vertical stress leads to an increase in the ε_v^{cr}.
- The volume change of specimens with high s_0 during SSL tests appears to be predominantly controlled by the state of suction stress rather than the applied vertical stress.
- During long-term creep tests at constant water content, a decrease in soil suction monitored by HCTs can be attributed to an increase in S_r of the specimen with decrease in total volume during creep. If this holds true, long-term creep tests where suction is artificially kept constant may not be ideal and the observed creep strains may not be solely attributed to the applied total vertical stress.
- Further investigations and more test results over a wider range of soil suction and applied vertical stress levels are required to validate the observed time-dependent response for the tested soil.

References

Alonso, E.E., Gens, A. and Josa, A. 1990. A constitutive model for partially saturated soils. Géotechnique, **40**(3): 405–430. doi: 10.1680/geot.1990.40.3.405.

Bagheri, M., Rezania, M. and Mousavi Nezhad, M. 2015. An experimental study of the initial volumetric strain rate effect on the creep behaviour of reconstituted clays. IOP Conference Series: Earth and Environmental Science, **26**(1): 012034.

Bagheri, M., Rezania, M. and Mousavi Nezhad, M. 2018. Cavitation in high-capacity tensiometers: effect of water reservoir surface roughness. Geotechnical Research, **5**(2): 81–95. doi: 10.1680/jgere.17.00016.

Bagheri, M., Mousavi Nezhad, M., and Rezania, M. 2019a. A CRS oedometer cell for unsaturated and non-isothermal tests. Geotechnical Testing Journal, **43**(1), in press. doi: 10.1520/GTJ20180204.

Bagheri, M., Rezania, M., and Mousavi Nezhad, M. 2019b. Rate-dependency and stress relaxation of unsaturated clays, International Journal of Geomechanics, In Press.

Cui, Y.-J., Le, T.T., Tang, A.M., Delage, P. and Li, X.L. 2009. Investigating the time-dependent behaviour of Boom clay under thermomechanical loading. Géotechnique, **59**(4): 319–329. doi: 10.1680/geot.2009.59.4.319.

De Gennaro, V., Delage, P., Cui, Y.J., Schroeder, C. and Collin, F. 2003. Time-dependent behavior of oil reservoir chalk: a multiphase approach. Soils and Foundations, **43**(4): 131–147. doi: 10.3208/sandf.43.4_131.

De Gennaro, V., Sorgi, C. and Delage, P. 2005. Air-water interaction and time dependent compressibility of a subterranean quarry chalk. Paper presented in Symposium Post Mining, Nancy, France, pp. 1–12.

Delage, P., Le, T.T., Tang, A.M., Cui, Y.J. and Li, X.L. 2007. Suction effects in deep Boom Clay block samples. Géotechnique, **57**(2): 239–244. doi: 10.1680/geot.2007.57.2.239.

578 Fredlund, D.G. and Xing, A. 1994. Equations for the soil-water characteristic curve. Canadian
579 Geotechical Journal, **31**(3): 521–532. doi: 10.1139/t94-061.
580 Fredlund, D.G. 2006. Unsaturated soil mechanics in engineering practice, Journal of Geotechnical
581 and Geoenvironmental Engineering, **132**(3): 286–321. doi: 10.1061/(ASCE)1090-
582 0241(2006)132:3(286)
583 Gasparre, A. 2005. Advanced labortory characterisation of London Clay. Ph.D. Thesis, University
584 of London.
585 Karstunen, M. and Yin, Z.-Y. 2010. Modelling time-dependent behaviour of Murro test
586 embankment. Géotechnique, **60**(10): 735–749. doi: 10.1680/geot.8.P.027.
587 Lai, X., Wang, S., Qin, H. and Liu, X. 2010. Unsaturated creep tests and empirical models for
588 sliding zone soils of Qianjiangping landslide in the Three Gorges. Journal of Rock
589 Mechanics and Geotechnical Engineering, **2**(2): 149–154. doi:
590 10.3724/SP.J.1235.2010.00149.
591 Li, J.Z., Peng, F.L. and Xu, L.S. 2009. One-dimensional viscous behavior of clay and its
592 constitutive modeling. International Journal of Geomechanics, **9**(2): 43–51. doi:
593 10.1061/(ASCE)1532-3641(2009)9:2(43).
594 Li, J.Z., Peng, F.L., Xu, L.S. and Tatsuoka, F. 2006. Viscous properties of clay with different
595 water content. Soil and rock behavior and modeling (GSP 150), ASCE, **194**: 55–61. doi:
596 10.1061/40862(194)6.
597 Li, J.-Z., Tatsuoka, F., Nishi, T. and Komoto, N. 2003. Viscous stress-strain behaviour of clay
598 under unloaded conditions. *In* Proceedings of the 3rd International Symposium on
599 Deformation Characteristics of Geomaterials: IS Lyon 03, Lyon, France, pp. 617–625.
600 Mataic, I., Wang, D. and Korkiala-Tanttu, L. 2016. Effect of destructuration on the compressibility
601 of Pernio clay in incremental loading oedometer tests. International Journal of
602 Geomechanics, **16**(1): 040150161. doi: 10.1061/(ASCE)GM.1943-5622.0000486.

Mesri, G. and Castro, A. 1987. C_α/C_c concept and K_0 during secondary compression. Journal of Geotechnical Engineering, **113**(3): 230–247. doi: 10.1061/(ASCE)0733-9410(1987)113:3(230).

Mesri, G. and Godlewski, P. M. 1977. Time and stress-compressibility interrelationship. Journal of Geotechnical Engineering Division, American Societry of Civil Engineeres, **103**(5): 417–430.

Mesri, G., Kwan, L.D.O., and Feng, W.T. 1994. Settlement of embankment on soft clays. *In* Proceedings of the Conference on Vertical and Horizontal Deformations of Foundations and Embankments: Part 2 (of 2), College Station, TX, USA, American Society of Civil Engineers, GSP 1(40), pp. 8–56.

Mesri, G. 2009. Discussion of 'Effects of friction and thickness on long-term consolidation behavior of Osaka Bay clays' by Watabe, Udaka, Kobayashi, Tabata & Emura 2008. Soils and Foundation., **49**(5): 823–824.

Monroy, R., Zdravkovic, L. and Ridley, A.M. 2008. Volumetric behaviour of compacted London Clay during wetting and loading. *In* Proceedings of the 1st European Conference on Unsaturated Soils, E-UNSAT 2008, Durham, UK, pp. 315–320.

Nazer, N.S.M., and Tarantino, A. 2016. Creep response in shear of clayey geo-materials under saturated and unsaturated conditions. *In* Proceedings of the 3rd European Conference on Unsaturated Soils, E-UNSAT 2016, Paris, France, pp. 1–5.

Oldecop, L.A., and Alonso, E.E. 2007. Theoretical investigation of the time-dependnet behaviour of rockfill. Géotechnique, **57**(3): 289–301. doi: 10.1680/geot.2007.57.3.289.

Pereira, J.M. and De Gennaro, V. 2010. On the time-dependent behaviour of unsaturated geomaterials. *In* Proceedings of the 5th International Conference on Unsaturated Soils, Barcelona, Spain, pp. 921–925.

627 Priol, G., De Gennaro, V., Delage, P. and Servant, T. 2007. Experimental investigation on the time
628 dependent behavior of a multiphase chalk. *In* Experimental unsaturated soil mechanics.
629 Edited by T. Schanz, Springer Proceedings Physics 112, pp. 161–167.
630 Rezania, M., Bagheri, M., Mousavi Nezhad, M. and Sivasithamparam, N. 2017. Creep analysis of
631 an earth embankment on soft soil deposit with and without PVD improvement. Geotextiles
632 and Geomembranes **45**(5): 537–547. doi: 10.1016/j.geotexmem.2017.07.004.
633 Sivakumar, V. 1993. A critical state framework for unsaturated soil. Ph.D. Thesis, University of
634 Sheffield, UK.
635 Sorensen, K.K. 2006. Influence of viscosity and ageing on the behaviour of clays. Ph.D. Thesis,
636 University College London.
637 Wheeler, S. J. and Sivakumar, V. 1995. An elasto-plastic critical state framework for unsaturated
638 soil. Géotechnique, **45**(1): 35–53. doi: 10.1680/geot.1995.45.1.35.
639 Yin, J.-H. and Feng, W.-Q. 2017. A new simplified method and its verification for calculation of
640 consolidation settlement of a clayey soil with creep. Canadian Geotechnical Journal, **54**(3):
641 333–347. doi: 10.1139/cgj-2015-0290.
642 Yin, Z.-Y., Karstunen, M., Chang, C.S., Koskinen, M. and Lojander, M. 2011. Modeling time-
643 dependent behavior of soft sensitive clay. Journal of Geotechnical and Geoenvironmental
644 Engineering, **137**(11): 1103–1113. doi: 10.1061/(ASCE)GT.1943-5606.0000527.
645 Zhou, A.N., Sheng, D., Sloan, S.W. and Gens, A. 2012. Interpretation of unsaturated soil
646 behaviour in the stress–saturation space, I: Volume change and water retention behaviour.
647 Computers and. Geotechnics, **43**: 178–187. doi: 10.1016/j.compgeo.2012.04.010.
648
649

Canadian Geotechnical Journal. Submitted 17 June 2018; accepted 27 June 2019.
https://doi.org/10.1139/cgj-2018-0398

List of Symbols

C_c = compression index in e – log σ'_v space
C_r = reloading index in e – log σ'_v space
C_s = swelling index in e – log σ'_v space
$C_{\alpha e}$ = creep index with respect to e
e = void ratio
e_0 = initial void ratio
e_i = instantaneous change in void ratio
e_p = void ratio 24 hours after the end of loading in SSL tests
G_s = specific gravity
I_p = plasticity index
k_v = coefficient of vertical permeability
m'_c = slope of compression curve in e – log σ_v space for unsaturated conditions
m_c = slope of compression curve in e – log σ'_v space for saturated conditions
S_r = degree of saturation
s = soil suction
s_0= initial suction
t = time
u_a = pore-air pressure
u_{exc} = excess pore-water pressure
u_w = pore-water pressure
w = gravimetric water content
w_0= initial gravimetric water content
w_L = liquid limit
w_P = plastic limit
α = represents the ratio $C_{\alpha e}/C_c$
β = represents the ratio e_i/e_p
ε_v^{cr} = volumetric creep strain
σ_p = yield vertical net stress in unsaturated states
σ'_p = yield vertical net stress in saturated states
σ_v = applied vertical total stress
σ'_v = vertical effective stress
σ_{vm} = maximum applied vertical stress
σ_{vnet} = net normal stress

Canadian Geotechnical Journal. Submitted 17 June 2018; accepted 27 June 2019.
https://doi.org/10.1139/cgj-2018-0398

652 **List of Tables**

653

654 **Table 1.** Physical properties of Sheppey London Clay samples

Clay (%)	Silt (%)	Sand (%)	*in-situ w* (%)	w_P (%)	w_L (%)	G_s	k_v (m/s) at 20° C
64	34	2	29 – 35	19 – 24	70 – 78	2.67	2.5×10^{-10}

655

Canadian Geotechnical Journal. Submitted 17 June 2018; accepted 27 June 2019.
https://doi.org/10.1139/cgj-2018-0398

656

Table 2. Details of MSL tests

Test ID	Loading/unloading stresses (kPa)	w_0 (%)	s_0 (kPa)	σ_{vm} (kPa)	Test duration (days)	Test condition
MSLis32-1	22-44-89-178-355-710-1421-710-355-178-89	32		1421	11	Saturated
MSLis32-2	22-44-89-178-355-710-1421-710-355-178-89	32		1421	11	
MSLis32-3	22-44-89-178-355-710-1421-710-355-178-89	32		1421	11	
MSLis32-4	11-22-44-89-178-222-333-444-666-888-1110-1332-1110-888-666-444-333-222-178	32		1332	19	
MSLis32-5	11-22-44-89-178-222-333-444-666-888-1110-1332-1110-888-666-444-333-222-178	32		1332	19	
MSLis32-6	11-22-44-89-178-222-333-444-666-888-1110-1332-1110-888-666-444-333-222-178	32		1332	19	
MSLis32-7*	22-44-89-133-178-222-333-444-666-888-1110-888-666-444-333-222-178-133	32		1110	18	
MSLis32-8*	22-44-89-133-178-222-333-444-666-888-1110-888-666-444-333-222-178-133	32		1110	18	
MSLis32-9*	22-44-89-133-178-222-333-444-666-888-1110-888-666-444-333-222-178-133	32		1110	18	
MSLrs39-1	11-22-44-89-178-355-710-1421-710-355-178-44	39		1421	12	
MSLrs39-2	11-22-44-89-178-355-710-1421-710-355-178-44	39		1421	12	
MSLrs39-3	11-22-44-89-178-355-710-1421-710-355-178-44	39		1421	12	
MSLrs43-1	11-22-44-89-178-355-710-1421-710-355-178-44	43		1421	12	
MSLrs43-2	11-22-44-89-178-355-710-1421-710-355-178-44	43		1421	12	
MSLrs43-3	11-22-44-89-178-355-710-1421-710-355-178-44	43		1421	12	
MSLru37	22-44-89-178-355-710-1110-710-355-178-89-44-22-11	37	326	1111	14	Unsaturated
MSLru36	22-44-89-178-355-710-1110-710-355-178-89-44-22-11	36	433	1111	14	
MSLru35	22-44-89-178-355-710-1110-710-355-178-89-44-22-11	35	513	1111	14	
MSLru28	25-50-100-200-300-400-500-580-500-400-300-200-100-50-25	28	1405	605	15	
MSLru26	25-50-100-200-300-400-500-580-500-400-300-200-100-50-25	26	1907	605	15	
MSLru15	25-50-100-200-300-400-500-580-500-400-300-200-100-50-25	15	~21000	605	15	

r: reconstituted, i: intact, s: saturated, u: unsaturated, *: low-quality undisturbed
The number before dash indicates initial water content and the number after dash indicates the test number.

657

Canadian Geotechnical Journal. Submitted 17 June 2018; accepted 27 June 2019.
https://doi.org/10.1139/cgj-2018-0398

658 **Table 3.** Details of SSL creep oedometer tests

Test ID	w_0 (%)	s_0 (kPa)	σ_{vm} (kPa)	Test duration (days)	Test conditions
SSLis32-178	32		178	37	Saturated
SSLis32-222	32		222	36	
SSLis32-355	32		355	36	
SSLis32-444	32		444	38	
SSLis32-666	32		666	38	
SSLrs39-178	39		178	60	
SSLrs39-222	39		222	68	
SSLrs39-355	39		355	68	
SSLrs39-444	39		444	46	
SSLrs39-666	39		666	46	
SSLrs43-355	43		355	94	
SSLrs43-444	43		444	94	
SSLru37-666	37	326	666	28	Unsaturated
SSLru37-444	37	326	444	29	
SSLru37-355	37	326	355	36	
SSLru36-666	36	433	666	28	
SSLru36-444	36	433	444	21	
SSLru36-355	36	433	355	34	
SSLru35-355	35	513	355	34	
SSLru35-222	35	513	222	34	
SSLru35-178	35	513	178	27	
SSLru28-666	28	1405	666	20	
SSLru28-444	28	1405	444	21	
SSLru28-355	28	1405	355	28	
SSLru26-222	26	1907	222	23	
SSLru26-178	26	1907	178	23	

The number after dash shows the σ_{vm}.

659

660

661

662

663

664

Canadian Geotechnical Journal. Submitted 17 June 2018; accepted 27 June 2019.
https://doi.org/10.1139/cgj-2018-0398

665

666 **Table 4.** Stress ranges for maximum C_c, $C_{\alpha e}$, and α parameters

Test ID	σ'_v / σ'_p or σ_v / σ_p			Range of α values	Average α
	$(C_c)_{max}$	$(C_{\alpha e})_{max}$	$(\alpha)_{max}$		
MSLis32-1 MSLis32-2 MSLis32-3	8 – 10	6 – 7	1 – 2	0.015 – 0.046	0.031 ± 0.016
MSLis32-4 MSLis32-5 MSLis32-6	8 – 10	8 – 11	1 – 2	0.017 – 0.031	0.024 ± 0.007
MSLis32-7* MSLis32-8* MSLis32-9*	6 – 8	4 – 5	4 – 5	0.023 – 0.048	0.036 ± 0.013
MSLrs39-1 MSLrs39-2 MSLrs39-3	3 – 4	6 – 7	1 – 2	0.022 – 0.037	0.03 ± 0.008
MSLrs43-1 MSLrs43-2 MSLrs43-3	3 – 4	3 – 4	1 – 2	0.024 – 0.036	0.03 ± 0.006
MSLru37 MSLru28 MSLru26	3 – 4	2 – 5	NA	0.023 – 0.037	0.03 ± 0.007
MSLru36 MSLru35 MSLru15	NA	NA	NA	0.023 – 0.045	0.034 ± 0.011

667